Electrochemical removal of bromate from drinking water

K. Matziaris[a], C. Polatides[b], I. Katsounaros[a], G. Kyriacou[a,*]

[a]*Department of Chemical Engineering, Aristotle University of Thessaloniki, Thessaloniki 54124, Greece*
Tel. +30 2310 996238; Fax: +30 2310 996196; email: kyriakou@eng.auth.gr
[b]*Department of Planning and Regional Development, University of Thessaly, Volos 38334, Greece*

ABSTRACT

The electrochemical removal of bromate on a tin cathode has been studied by both electrochemical techniques, such as cyclic voltammetry and chronoamperometry, as well as by steady-state electrolytic experiments. The reduction of bromate in 2 M NaCl takes place efficiently at potentials more negative than −1.4 V vs. Ag/AgCl and the rate of the reduction displays a maximum at about −1.8 V, then decreases and consequently it increases again as the potential becomes more negative than −1.9 V. The % removal efficiency of bromate displays a maximum (75.6%) at −1.8 V, while the % selectivity of bromide displays a minimum (70.3%) at the same potential.

Keywords: Bromate; Electrochemical; Removal; Reduction; Tin cathode

1. Introduction

The use of ozone for the disinfection of water is a safe and environmentally friendly method. However, during the disinfection of water by ozonation a part of the Br^-, which is naturally contained in the water in concentrations ranged from 10 to $100 \, \mu g \, L^{-1}$, is oxidized to bromate through the reactions [1]:

$$O_3 + Br^- \rightarrow O_2 + BrO^- \tag{1}$$

$$2O_3 + BrO^- \rightarrow 2O_2 + BrO_3^- \tag{2}$$

In addition, bromate may also be formed in concentrated hypochlorite solutions which are also used for the disinfection of drinking water [2]. The World Health Organization has classified bromate in the Group 2B as a "possible human carcinogen" [3], even though there is not any study in humans so far. Many countries have implemented regulations in which the maximum contaminant level (MCL) in potable water was set to $10 \, \mu g \, L^{-1}$ [4].

Many methods for the removal of bromate from potable water have been proposed including ion exchange [5], nanofiltration [6], UV irradiation [7], photocatalytic degradation [8], coagulation with Al^{3+} and Fe^{3+} [9], chemical reduction with a variety of reducing agents, such as Fe^{2+} [10], biological degradation [11], as well as electrochemical reduction on various cathodes [12–15].

Bromate has been used as a model anion since 1960 by many researchers, in studies regarding the electron transfer to anionic species [16,17]. These studies have

*Corresponding author.

been performed by electrochemical techniques and as far as we know there are no works in the literature performed by steady-state electrolysis containing the analysis of all the species produced during the electrolysis, apart from a recent work by Zhao et al. [13] on boron-doped diamond (BDD) cathode. It should be noted that the analytical determination of the products of the reduction has a crucial importance since the possible by-products of the reduction can be more toxic than the reduced bromate. Tin has been proved to be an efficient cathode for the electrochemical reduction of nitrate and nitrite [18]. In this study, we present experimental results on the electrochemical reduction of bromate on a tin cathode performed by both electrochemical techniques as well as by steady-state electrolytic experiments.

2. Experimental

The cyclic voltammetry experiments were performed in a three-compartment glass cell equipped with a Ag/AgCl sat. KCl as reference. The cathode was a Sn foil (Sigma–Aldrich, 99.9%) of $0.6\,cm^2$ and the anode was a platinized Pt foil (Alpha–Metal) of $6\,cm^2$. The potential was controlled by a Wenking POS73 (Bank-Elektronik) potentiostat and the voltammograms were recorded by a DUO18 (World Precision Instruments) software. The steady-state electrolysis experiments were performed in a cell constructed by Teflon, which was equally divided into two volumes (10 mL) by a Nafion 117 (H^+ form) cation exchange membrane.

The cathode was a foil of a Sn having a geometric area of $7\,cm^2$ and the anode was a platinized Pt foil (Alpha Metal) of equal area. The working electrode was polished before each experiment by a Struers DP–U2 grinding equipment with a No. 1200 polishing paper and subsequently rinsed with ultra-pure water. The solution of the catholyte was degassed for about 10 min by He and then the desirable potential was applied.

The concentration of bromate was determined by a DIONEX 4500i ion chromatograph using an AS-19 column (eluent: 0.02 M KOH with 1 mL/min) and the detection was performed by a suppressed conductivity detector. Under these conditions, the analytical method enabled the determination of bromide and bromate in concentrations lower than $0.005\,mg\,L^{-1}$ according to the reference chromatograms given by Dionex [19].

3. Results and discussion

3.1. Study by cyclic voltammetry

A cyclic voltammogram for the reduction of 0.2 M $NaBrO_3$ in 2 M NaCl is shown in Fig. 1. A quasi-
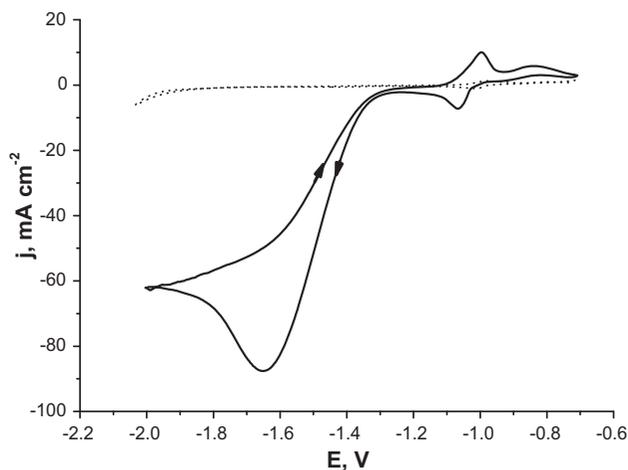
Fig. 1. Cyclic voltammogram of $0.2\,M\ NaBrO_3 + 2\,M\ NaCl$ on Sn. The dotted line represents the background current. Scan Rate: $20\,mV\,s^{-1}$.

reversible wave at $E_{mid} = -1.1\,V$ and an irreversible reduction wave at $E_p = -1.7\,V$ were observed. The peak $E_{mid} = -1.1\,V$ has been already observed by other researchers in corrosion studies performed in sulfate-containing electrolytes and was attributed to oxidation/reduction of surface species of tin [20].

The peak at about $-1.7\,V$ vs. Ag/AgCl was attributed to the reduction of bromate. The peak current increases proportionally with the square root of the scan rate and this proves that it is a diffusion wave (Fig. 2). The current density of the reduction of bromate in both potential regions increases as the concentration of bromate increases (Fig. 3). The irreversible peak current (at about $-1.7\,V$ vs. Ag/AgCl) is proportional to the concentration of bromate (inset).
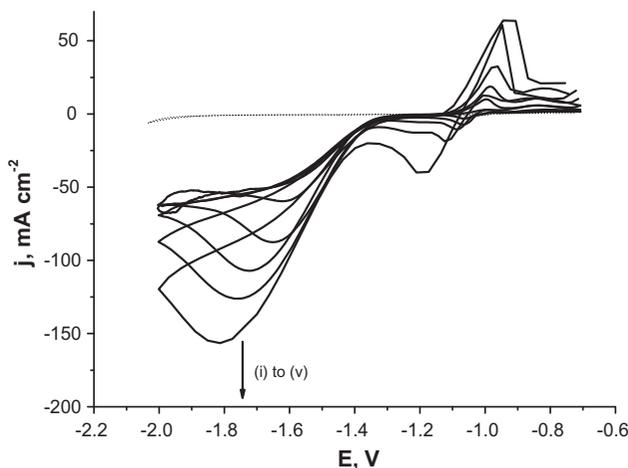
Fig. 2. Cyclic voltammograms of $0.2\,M\ NaBrO_3 + 2\,M\ NaCl$ on Sn. Scan rates: (i) 5, (ii) 20, (iii) 50, (iv) 100, and (v) $200\,mV\,s^{-1}$. Dotted line represents the background.
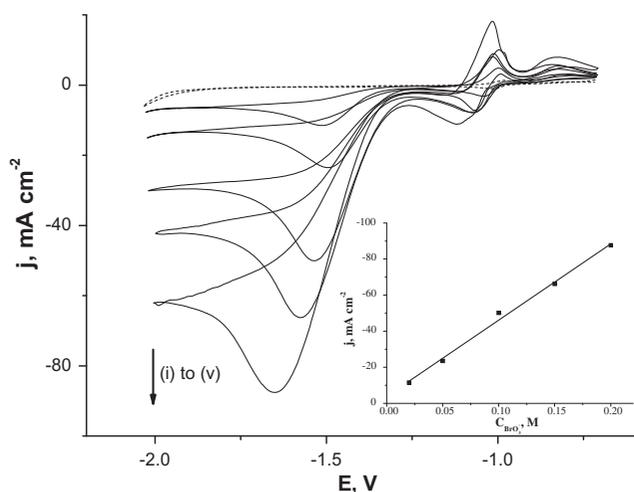
Fig. 3. Cyclic voltammograms of (i) 0.02, (ii) 0.05, (iii) 0.1, (iv) 0.15, and (v) 0.2 M NaBrO₃ + 2 M NaCl on Sn. Scan Rate: 20 mV s⁻¹. Dotted line represents the background current. The inset shows the peak current of the irreversible wave vs. concentration of bromate.

The logarithm of the peak current density is expected to be linearly depended on the logarithm of the concentration of bromate and the slope of this diagram represents the reaction order [21], because:

$$j = (n\,F)\,r = (n\,F)\,k\,C^v => \log j = v \log C + \log(n\,F k) \tag{3}$$

where j is the current density, n is the number of the electrons exchanged, F is the Faraday constant, r is the reaction rate, k is the rate constant, C is the concentration of the reactant, and v is the reaction order. Fig. 4 shows that the logarithm of the current density is
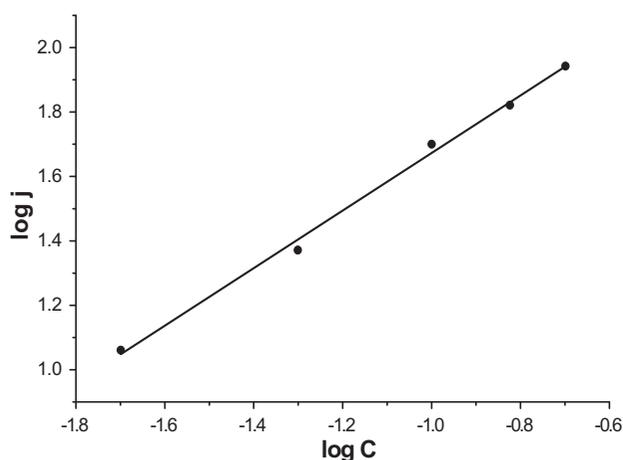
Fig. 4. Logarithm of the peak current density vs. the logarithm of the concentration of bromate, during the cyclic voltammograms presented in Fig. 3.

proportional to the logarithm of the concentration of bromate based on the cyclic voltammograms of Fig. 3. The slope of this diagram was found to be $v = 0.9$, which means that the reduction of bromate follows about first-order kinetics.

3.2. Study by chronoamperometry

Fig. 5 shows the chronoamperometric curves obtained in solutions with different concentrations of bromate. The potential was initially set at −1.0 V for 1 min and then a potential of −1.8 V was applied. Thereafter, the current was recorded vs. time until a plateau was reached. The current density decreases with time, as it is expected from the Cottrell equation [21]:

$$i(t) = n\,FA\sqrt{\frac{D}{\pi t}}\,C_0^* \tag{4}$$

where $i(t)$ is the current vs. time, n is the number of electrons, F is the Faraday constant, A is the electrode area, D is the diffusion coefficient of the reactant, t is the time after applying the potential, and C_0^* is the bulk concentration of the reactant.

The Cottrell equation can be simplified as follows:

$$i(t) = kt^{-1/2}, \quad \text{where } k = nFA\sqrt{\frac{D}{\pi}}\,C_0^* \tag{5}$$

Eq. (5) predicts that the current density depends on $t^{-1/2}$. The chronoamperometric curves, shown in
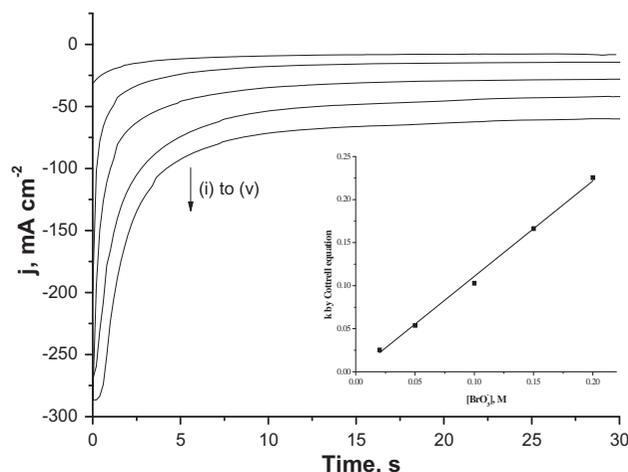
Fig. 5. Chronoamperometric curves obtained in 2 M NaCl⁺ (i) 0.02, (ii) 0.05, (iii) 0.1, (iv) 0.15, and (v) 0.2 M NaBrO₃. The potential was initially set at −1.0 V vs. Ag/AgCl for 1 min and then a potential of −1.8 V vs. Ag/AgCl was applied for 30 s. The inset shows the dependence of the constant k obtained by the Cottrell equation (Eq. (5)) on the concentration of bromate.

Fig. 5, can be reliably simulated using Eq. (5) and a k value can be obtained for each concentration of bromate. The inset shows that the k obtained by the Cottrell equation is linearly dependent on the concentration of bromate, as it is expected from Eq. (5).

According to Eq. (5), the slope of the diagram of k vs. the concentration of bromate is equal to $nFAD^{1/2}\pi^{1/2}$. Therefore, the number of the electrons exchanged, n, can be calculated from the slope of the diagram of the inset. The slope of the diagram of k vs. the concentration of bromate was 1.1, the diffusion coefficient of bromate in a 2 M NaCl solution is $D = 1.09 \times 10^{-5}$ cm^2/s [22], and the surface area of the electrode was $A = 0.6$ cm^2. By this way, n was found to be 6.16 and this means that at -1.8 V vs. Ag/AgCl, bromate is mainly reduced to bromide through the total reaction:

$$BrO_3^- + H_2O + 6e^- \rightarrow Br^- + 6OH^- \tag{6}$$
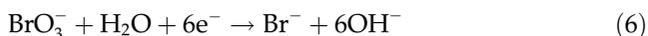
3.3. Steady-state electrolytic experiments

Fig. 6 shows the concentration profile of bromate and bromide and the mass loss during the electrolysis time at -1.6 V vs. Ag/AgCl. The concentration of bromate follows a sigmoidal form in which the rate of the reduction is low at the first electrolysis steps and then increases, while the concentration of bromide displays a reverse sigmoidal curve. The shape of this curve may be attributed to the shift of the interfacial pH to higher values due to the hydroxyl anions which are produced during the electrolysis through the reaction (6). A similar behavior was observed by Frumkin

many years ago [23] and was attributed to the acceleration of the reduction of bromate at pH values higher than 12.

The total mass balance of bromine shows that there is a mass loss during the electrolysis which displays a maximum after 150 min. The maximum loss in the mass balance corresponded to the 8.7% of the initial concentration of bromine. The form of this curve implies that a consecutive reaction mechanism takes place. The presence of an intermediate was verified from the chromatogram (Fig. 7) which showed a new peak at about 17 min apart from that of bromate, chloride, and bromide at 5.7, 7.5, and 10 min, respectively. This peak was attributed to the hypobromite anion (BrO$^-$), but it cannot be proved because BrO$^-$ is unstable in aqueous solution and, thus, a standard solution cannot be reliably prepared. It should be noted that the chemistry of the bromine acids in aqueous solutions is complicated and can include many reactions [24]:

$$BrO_3^- + e^- + H_2O \rightarrow BrO_2^- + OH^- \tag{7}$$

$$2BrO_2^- \rightarrow BrO_3^- + BrO^- \tag{8}$$

$$BrO^- + BrO_2^- \rightarrow BrO_3^- + Br^- \tag{9}$$

$$Br^- + BrO_2^- \rightarrow 2BrO^- \tag{10}$$

$$2BrO^- \rightarrow Br^- + BrO_2^- \tag{11}$$
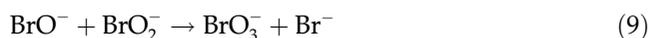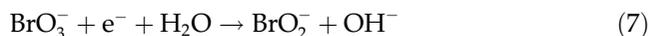
The above reaction scheme shows that the initial bromate which is reduced by the reaction (7) can be reproduced from the reactions (8) and (9). The presented scheme of the reduction can explain why the kinetics is more complicated than that predicted

Fig. 6. Concentration profile of bromate (▲), bromide (●), and the mass loss (■) during the electrolysis time at -1.6 V vs. Ag/AgCl. Initial solution 0.1 M NaBrO$_3$ + 2 M NaCl.
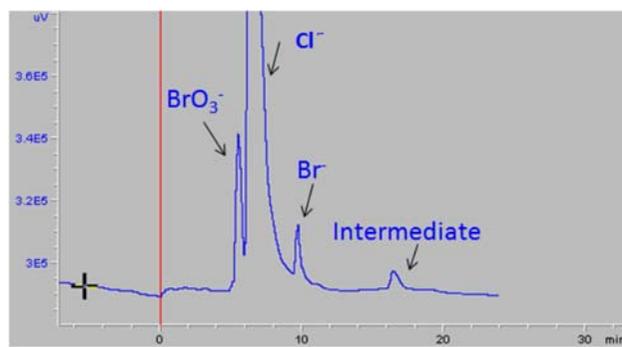
Fig. 7. A typical chromatogram obtained during the electrolysis of a solution 0.1 M NaBrO$_3$ + 2 M NaCl at -1.6 V. Electrolysis time 45 min.

by the voltammetric measurements (Fig. 4). The experimental results of the present work cannot be modeled by consecutive reaction kinetics because the concentration of the intermediate cannot be determined exactly due to its instability. However, Zhao et al. [13] observed that the reduction of bromate follows first-order kinetics, but in their case the concentration of bromate was much lower than that of our work. The lower concentration leads to a lower rate of production of hydroxyls according to the reaction (6) and, therefore, to a lower shift of the interfacial pH possibly at values lower than 12.

Fig. 8 shows the % removal efficiency (%RE) of bromate, the % selectivity (%S) of bromide, and the mean rate of the reduction vs. the applied potential at electrolysis time 180 min. The %RE of bromate displays a maximum (75.6%) at −1.8 V and then decreases, which is possibly due to the repulsion of bromate from the likely charged electrode. The %S of bromide was ranged between 70 and 93% displaying a minimum (70.3%) at −1.8 V. The curve of the mean rate of the reduction vs. potential displayed a similar form to that of the %RE having a maximum (0.00048 M min^{-1}) at −1.8 V. Even though the final concentration of bromate in our work is much higher than the MCL (10 μg L^{-1}), this method can be applied in natural waters by using deposited tin on porous electrodes, which have much higher electrochemically active surface area than a tin foil. The produced intermediate is unstable and decomposes rapidly to bromide [24] and, thus, it cannot affect the quality of the produced water.

However, the RE of bromate (∼76%) is lower than the achieved by Zhao et al. [13] on BDD, but the concentration of bromate was much lower than that in our experiments. A higher %RE on tin could be
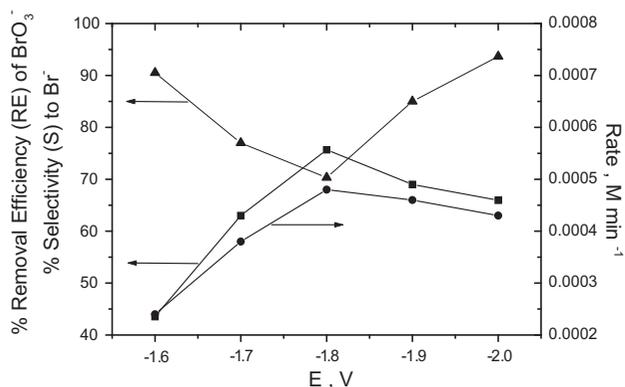
achieved if the electrolysis continued for a longer time. It should be mentioned that in our case the current efficiency of the process was about 100% since the hydrogen evolution reaction on tin is negligible at −1.8 V.

4. Conclusions

The present study showed that tin is a promising cathode for the electrochemical reduction of bromate (BrO$_3^-$), aiming to the removal of bromate ions from drinking water which are produced from the disinfection treatment by ozonation. The rate of the reduction displays a maximum at −1.8 V. A mass loss of bromine balance was attributed to the produced bromite (BrO$_2^-$) and hypobromite (BrO$^-$) which are unstable anions, while the main product of the reduction is bromide (Br$^-$). Although cyclic voltammetry predicted first-order kinetics for the electrochemical reduction of bromate to bromide, the steady-state electrolytic experiments showed that the concentration profile of bromate displays a sigmoidal form.

References

[1] U.V. Gunten, Ozonation of drinking water: Part II disinfection and by-product formation in presence of bromide, iodide or chlorine, Water Res. 37 (2003) 1469–1487.
[2] IPCS, Disinfectants and Disinfectant By-Products, World Health Organization, International Programme on Chemical Safety, Environmental Health Criteria 216, WHO, Geneva, 2000.
[3] Y. Kurokawa, A. Maekawa, M. Takahashi, Y. Hayashi, Toxicity and carcinogenicity of potassium bromate—a new renal carcinogen, Environ. Health Perspect. 87 (1990) 309–335.
[4] European Union, Relating to the Quality Intended for Human Consumption. Directive 98/83/EC, (1998).
[5] C.T. Matos, S. Velizarov, M. Reis, J.G. Crespo, Removal of bromate from drinking water using the ion exchange membrane bioreactor concept, Environ. Sci. Technol. 42 (2008) 7702–7708.
[6] M.J. Prados-Ramirez, N. Ciba, M.M. Bourbigot, Available techniques for reducing bromate in drinking water, Water Supply 13 (1995) 61–70.
[7] S. Peldszus, S.A. Andrews, R. Souza, F.D. Smith, I. Douglas, J. Bolton, P.M. Huck, Effect of medium-pressure UV irradiation on bromate concentrations in drinking water, a pilot-scale study, Water Res. 38 (2004) 211–217.
[8] H. Noguchi, A. Nakajima, T. Watanabe, K. Hashimoto, Design of a photocatalyst for bromate decomposition: Surface modification of TiO$_2$ by pseudo-boehmite, Environ. Sci. Technol. 37 (2003) 153–157.
[9] R. Butler, A.R. Godey, R. Lake, L. Lytton, E. Cartmell, Reduction of bromate in groundwater with an ex-situ suspended growth bioreactor, Water Sci. Technol. 52 (2001) 265–273.
[10] M. Siddiqui, G. Amy, K. Ozekin, W. Zhai, P. Westerhoff, Alternative strategies for removing bromate, J. Am. Water Works Assn. 86 (1994) 81–96.
[11] M. Kirisits, V. Snoeyink, J. Chee-Sanford, B. Daugherty, J. Brown, L. Raskin, Effect of operating conditions on bromate removal efficiency in BAC filters, J. Am. Water Works Assn. 94 (2002) 182–193.

Fig. 8. Percent RE of bromate (■), % Selectivity of bromide (▲) (left axis), and rate (●) (right axis) of the reduction vs. the applied potential at electrolysis time 180 min. Initial solution. 0.1 M NaBrO$_3$ + 2 M NaCl.

[12] S. Dong, L. Cheng, X. Zhang, Electrochemical studies of a lanthanide heteropoly tungstate/molybdate complex in polypyrrole film electrode and its electrocatalytic reduction of bromate, Electrochim. Acta 43 (1998) 563–568.

[13] X. Zhao, H. Liu, A. Li, Y. Shen, J. Qu, Bromate removal by electrochemical reduction at boron-doped diamond electrode, Electrochim. Acta 62 (2012) 181–184.

[14] P. Wang, X. Wang, G. Zhu, PMo_{12}—doped carbon ceramic composite electrode based on sol-gel chemistry and ist electrocatalytic reduction of bromate, Electroanal. 12 (2000) 1493–1497.

[15] G.E. Badea, T. Badea, Kinetics and mechanism of the bromate electrochemical reduction at platinum electrode, Rev. Roumaine Chim. 51 (2006) 127–133.

[16] P. Delahay, M. Kleinerman, Structure of the double layer and electrode processes II: Effect of the nature of the electrode and application of the thallium-amalgam electrode, J. Am. Chem. Soc. 82 (1960) 4509–4513.

[17] V.A. Benderskii, A.G. Krivenko, N.V. Fedorovich, Photocurrent kinetics during electron emission from a metal into an electrolyte solution: Part IX. Electrode reactions of the intermediates generated in the bromate ion reduction on mercury, J. Electroanal. Chem. 241 (1988) 265–279.

[18] I. Katsounaros, D. Ipsakis, C. Polatides, G. Kyriacou, Efficient electrochemical reduction of nitrate to nitrogen on tin cathode at very high cathodic potentials, Electrochim. Acta 52 (2006) 1329–1338.

[19] http://www.dionex.com/en-us/products/columns/ic-rfic/hydroxide-selective-packed/ionpac-as19/lp-73262.html.

[20] S.S. Abd El-Rehim, F. Taha, M.B. Saleh, S.A. Mohamed, On the pitting corrosion of tin by sulphate anion, Corros. Sci. 33 (1992) 1789–1796.

[21] A.J. Bard, L.R. Faulkner, Electrochemical Methods: Fundamentals and Applications, second ed., Wiley, New York, NY, 2001.

[22] R.C. Reid, J.M. Prausnitz, B.E. Poling, The Properties of Gases and Liquids, fourth ed., McGraw Hill, New York, NY, 1987.

[23] A.N. Frumkin, Influence of cation adsorption on the kinetics of electrode processes, Trans. Faraday Soc. 55 (1959) 156–167.

[24] C.L. Lee, M.W. Lister, The decomposition of aqueous sodium bromite, Can. J. Chem. 49 (1971) 2822–2826.